Supporting Information for

A Chlorin-Based Nanoscale Metal-organic Framework for Photodynamic Therapy of Colon Cancers

Kuangda Lu[†], Chunbai He[†], and Wenbin Lin*

Department of Chemistry, University of Chicago, 929 E 57th St, Chicago, IL 60637, USA

Table of Contents

1. Materials and cell lines

All of the starting materials were purchased from Sigma-Aldrich and Fisher (USA), unless otherwise noted, and used without further purification.

Murine colon adenocarcinoma cell CT26 and human colorectal adenocarcinoma HT29 were purchased from the American Type Culture Collection (Rockville, MD, USA) and cultured in RPMI 1640 medium and Dulbecco's Modified Eagle's Medium (DMEM) medium (Gibco, Grand Island, NY, USA) supplemented with 10% FBS, respectively.

Athymic male nude mice (6 weeks, 24-26 g) and BALB/c male mice (6 weeks, 22-24 g) were provided by Harlan Laboratories, Inc (USA). The study protocol was reviewed and approved by the Institutional Animal Care and Use Committee (IACUC) at the University of Chicago.

2. Synthesis of 5,15-di(p-benzoato)chlorin (H_2DBC)

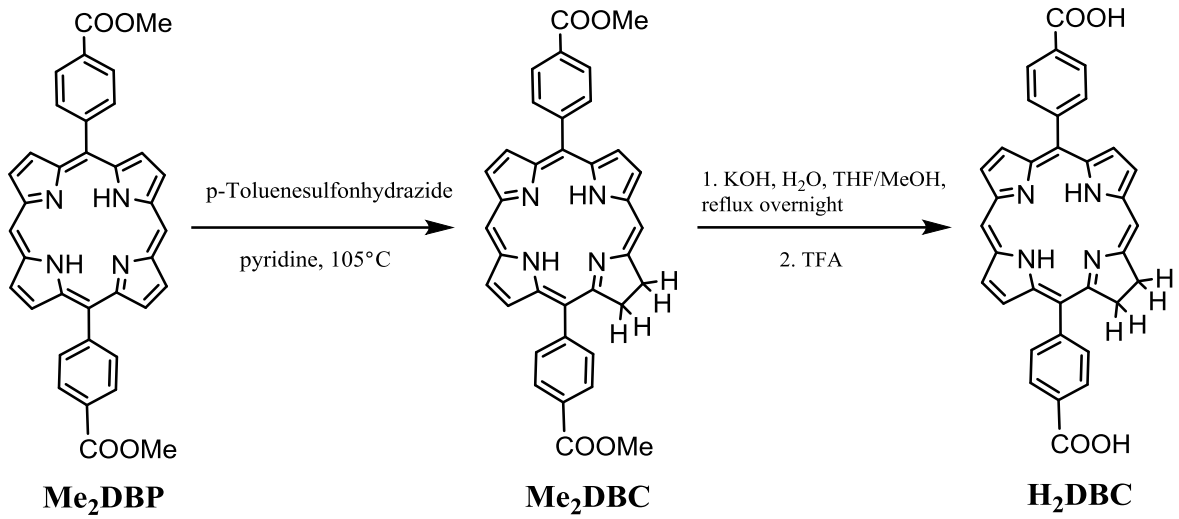

Scheme S1. Synthesis of the 5,15-di(p-benzoato)chlorin ligand (H_2DBC).

5,15-di(p-methylbenzoato)porphyrin (Me_2DBP) was synthesized as previously reported.[1] Me_2DBP was reduced to 5,15-di(p-methylbenzoato)chlorin (Me_2DBC) following a modified procedure from the literature.[2] To a 2-neck round bottom flask were added Me_2DBP (239 mg, 0.41 mmol) and anhydrous potassium carbonate (520 mg, 3.76 mmol). Under nitrogen protection 30 mL of anhydrous pyridine was added. The solution was heated to 105 °C before the addition of 3 mL of p-toluenesulfonhydrazide solution (0.275 M in anhydrous pyridine). The reaction mixture was kept at 105 °C for another 8 hours during which 4 fractions of p-toluenesulfonhydrazide solutions (0.275 M in anhydrous pyridine, 3 mL for each fraction) were added every 2 h. The reaction mixture was then stirred at 105 °C in the dark for another 12 h. The product was extracted with 2:1 ethyl acetate/water and washed with 2 M HCl, 2 M phosphoric acid (twice), water, and saturated sodium bicarbonate solution. The solution was treated with 2,3-dichloro-5,6-dicyano-benzoquinone (via slow addition of 1 mg/mL solution in chloroform) until the characteristic absorption of the over-reduced product at 735 nm disappeared. Silica gel chromatography with chloroform as eluent afforded pure Me_2DBC. Yield: 26% (62 mg, 0.11 mmol). ^{1}H-NMR (500 MHz, chloroform-D, ppm): δ=9.89 (s, 1H), 9.14 (dd, 1H), 9.06 (s, 1H), 8.99 (d, 1H), 8.85 (d, 1H), 8.77 (d, 1H), 8.59 (d, 1H), 8.44 (t, 4H), 8.35 (dd, 1H), 8.27 (d, 2H), 8.04 (d, 2H), 4.72 (t, 2H), 4.36 (t, 2H), 4.13 (s, 3H), 4.12 (s, 3H), -1.42 (s, 1H), -1.91 (s, 1H). ESI-MS for $[Me_2DBC+H]^+$: 581.1 calcd; 581.2 found.

a)

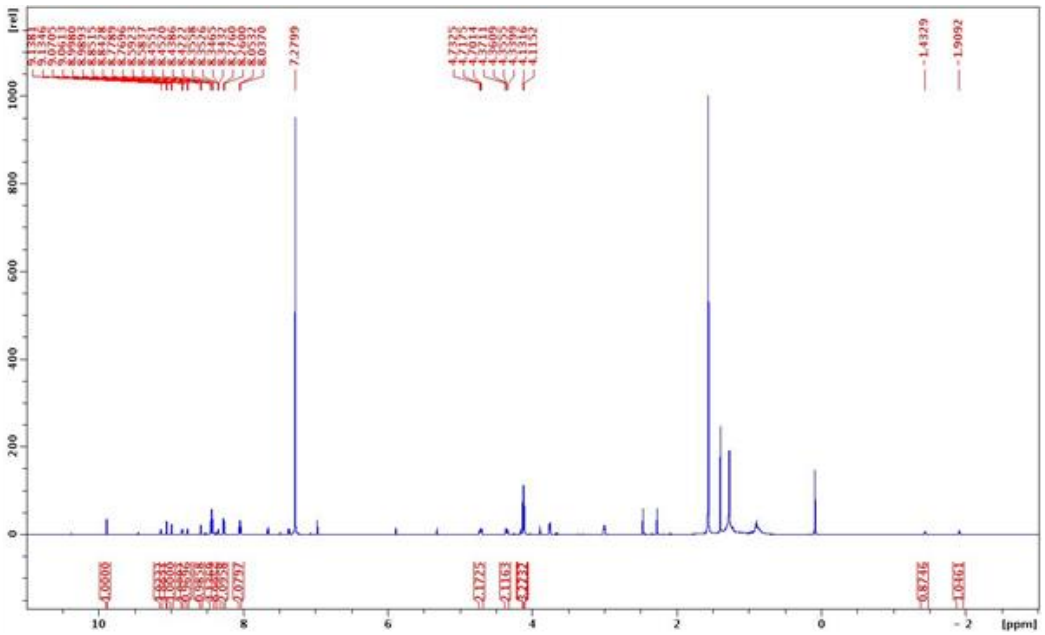

b)

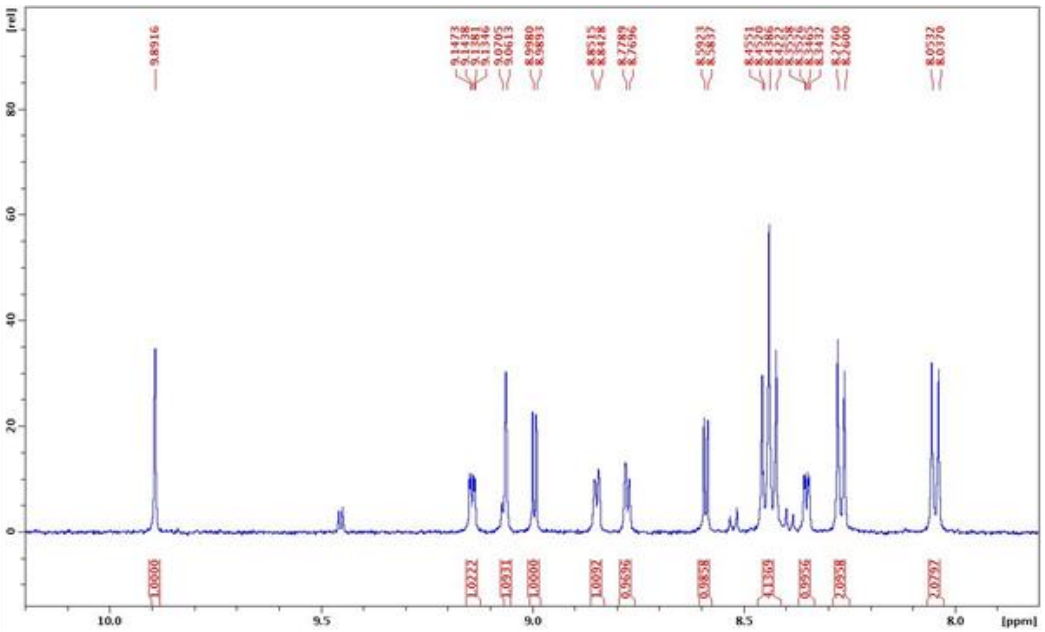

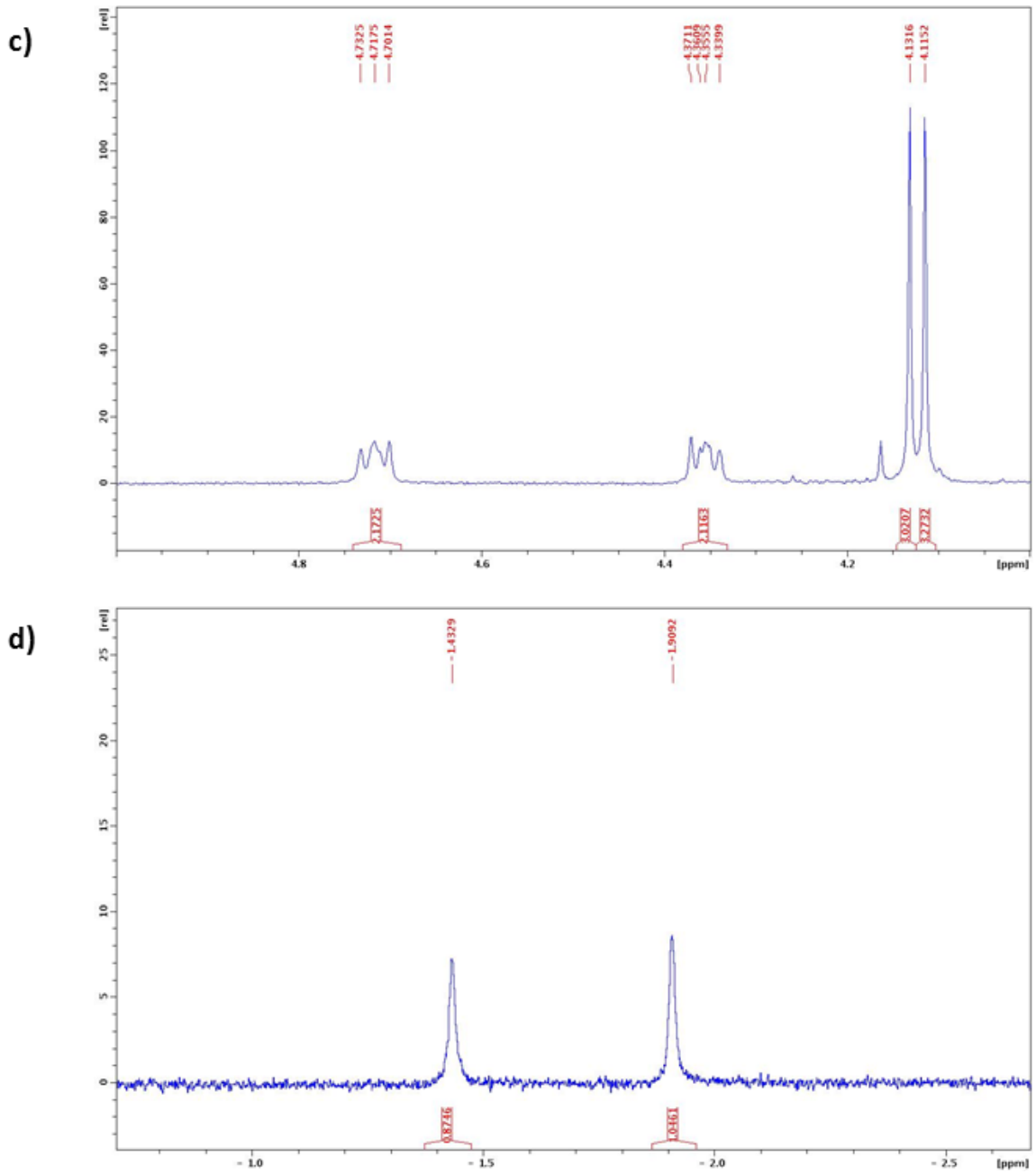

Figure S1 a) ^{1}H NMR spectrum of 5, 15-di(p-methyl-benzoato)chlorin in chloroform-D. b-d) expanded view of different portions of the spectrum.

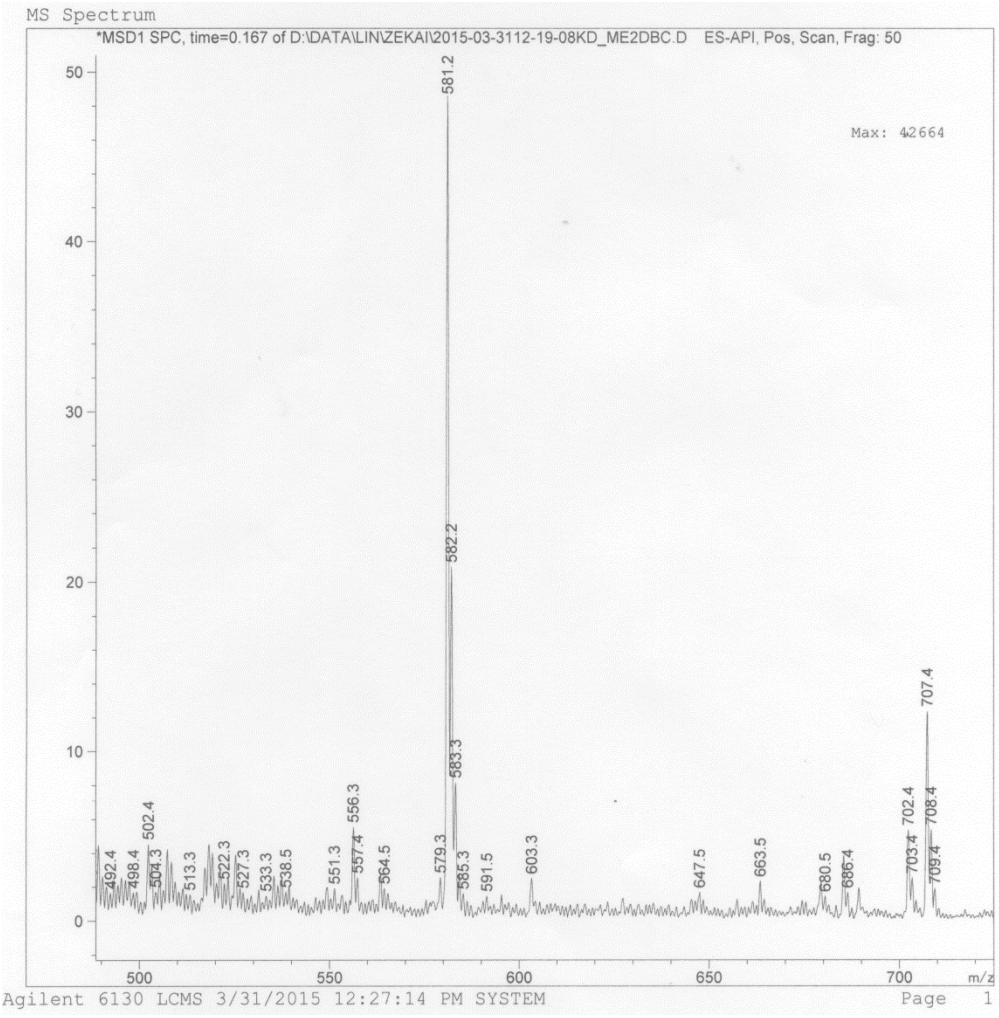

Figure S2 ESI-MS of 5, 15-di(p-methylbenzoato)chlorin. The sample was prepared in dichloromethane as a 40 mg/L solution and was delivered by dichloromethane.

Me_2DBC (62 mg, 0.11 mmol) was dissolved in a mixture of tetrahydrofuran (THF) and methanol (24 mL, 1:1 vol/vol). A potassium hydroxide aqueous solution (2.5 mL, 2 mol/L) was then added. The solution was heated to reflux under nitrogen protection overnight. Half of the solvent was removed by a rotary evaporator before the pH was adjusted to pH=3 with the addition of trifluoroacetic acid. The dark brownish product was collected by vacuum filtration, washed with water and ether, and dried under vacuum to afford the desired product in 88% yield (52 mg, 0.094 mmol). ^{1}H-NMR (500 MHz, DMSO-D_6, ppm): δ=13.25 (s, 2H), 10.11 (s, 1H), 9.40 (d, 1H), 9.28 (s, 1H), 9.08 (m, 2H), 8.79 (d, 1H), 8.48 (d, 1H), 8.35 (m, 5H), 8.27 (d, 2H), 8.12 (d, 2H), 4.70 (t, 2H), 4.32 (t, 2H), -1.50 (s, 1H), -2.03 (s, 1H). ESI-MS for $[H_2DBC+H]^+$: 553.1 calcd; 553.2 found.

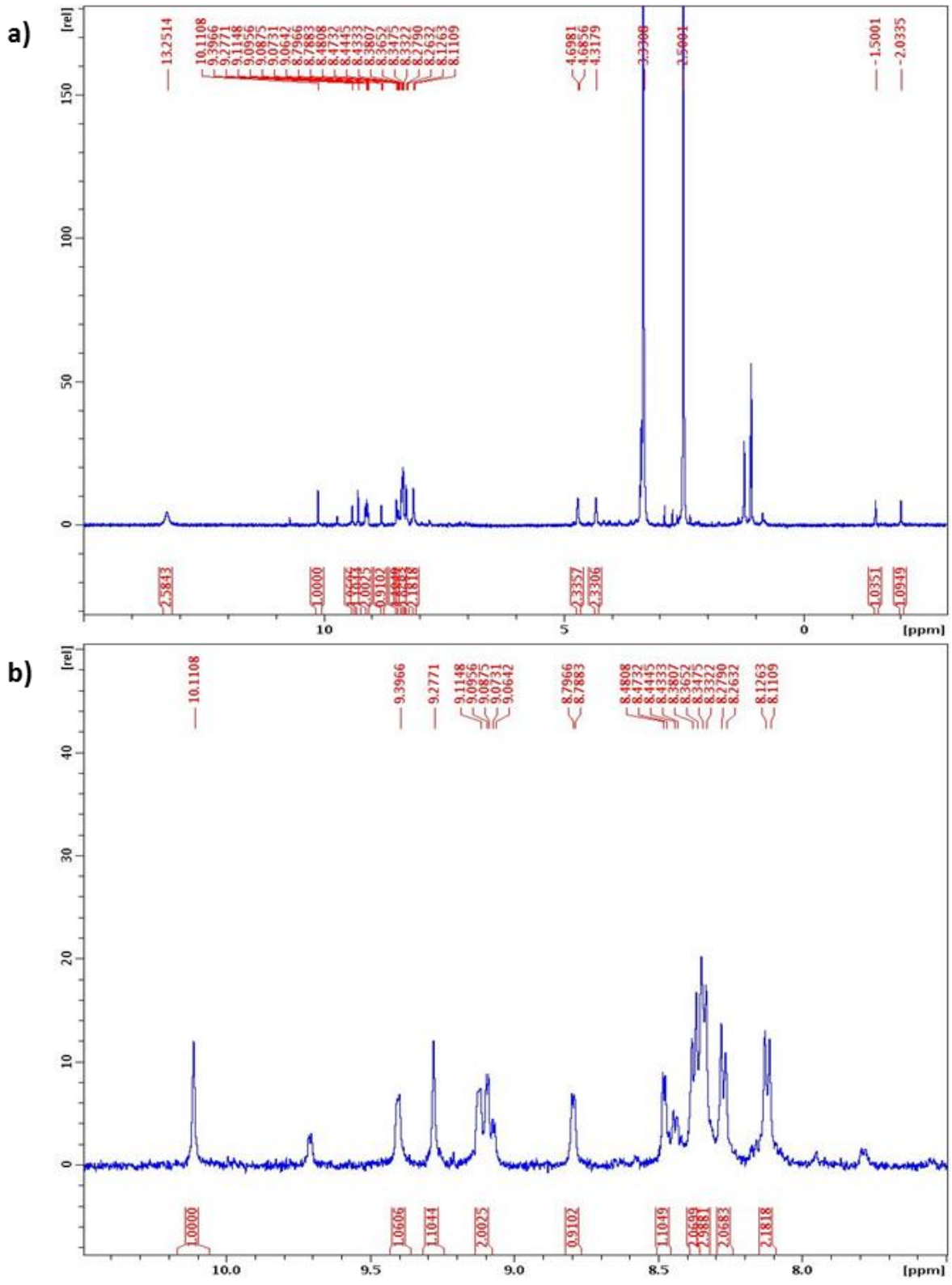
a)
[rel]
13.2514
10.1108
9.3966
9.2771
9.1148
9.0956
9.0875
9.0731
9.0642
8.7966
8.7883
8.4808
8.4732
8.4445
8.4333
8.3807
8.3652
8.3475
8.3322
8.2790
8.2632
8.1263
8.1109
4.6981
4.6856
4.3179
3.3300
2.5001
-1.5001
-2.0335
2.5843
1.0000
1.0606
1.1044
2.0025
0.9102
1.1049
2.0689
2.9881
2.0683
2.1818
0.3357
0.3306
0.0351
1.0949
[ppm]
b)
[rel]
10.1108
9.3966
9.2771
9.1148
9.0956
9.0875
9.0731
9.0642
8.7966
8.7883
8.4808
8.4732
8.4445
8.4333
8.3807
8.3652
8.3475
8.3322
8.2790
8.2632
8.1263
8.1109
1.0000
1.0606
1.1044
2.0025
0.9102
1.1049
2.0689
2.9881
2.0683
2.1818
[ppm]

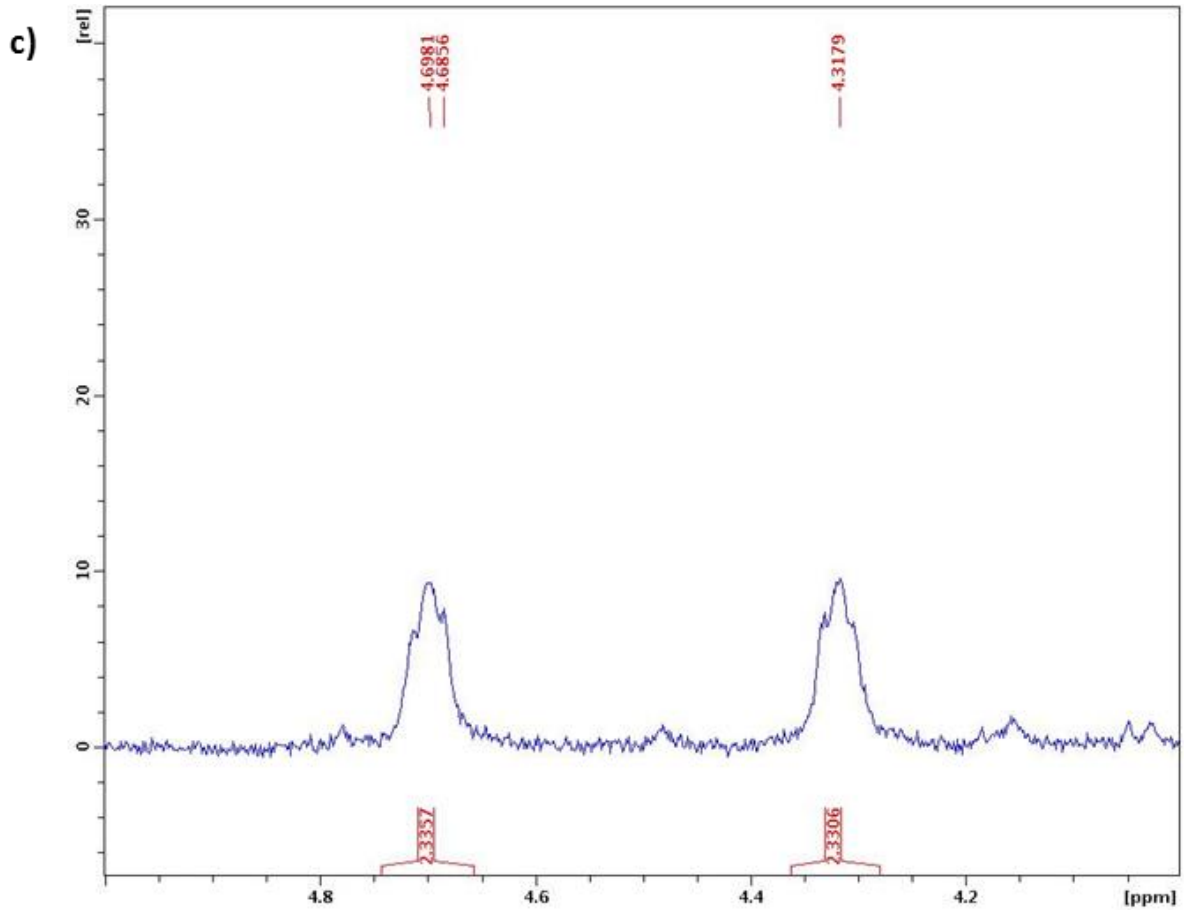

Figure S3 a) ^{1}H NMR spectrum of 5, 15-di(p-benzoato)porphyrin in DMSO-D_6. b,c) expanded view of portions of the spectrum.

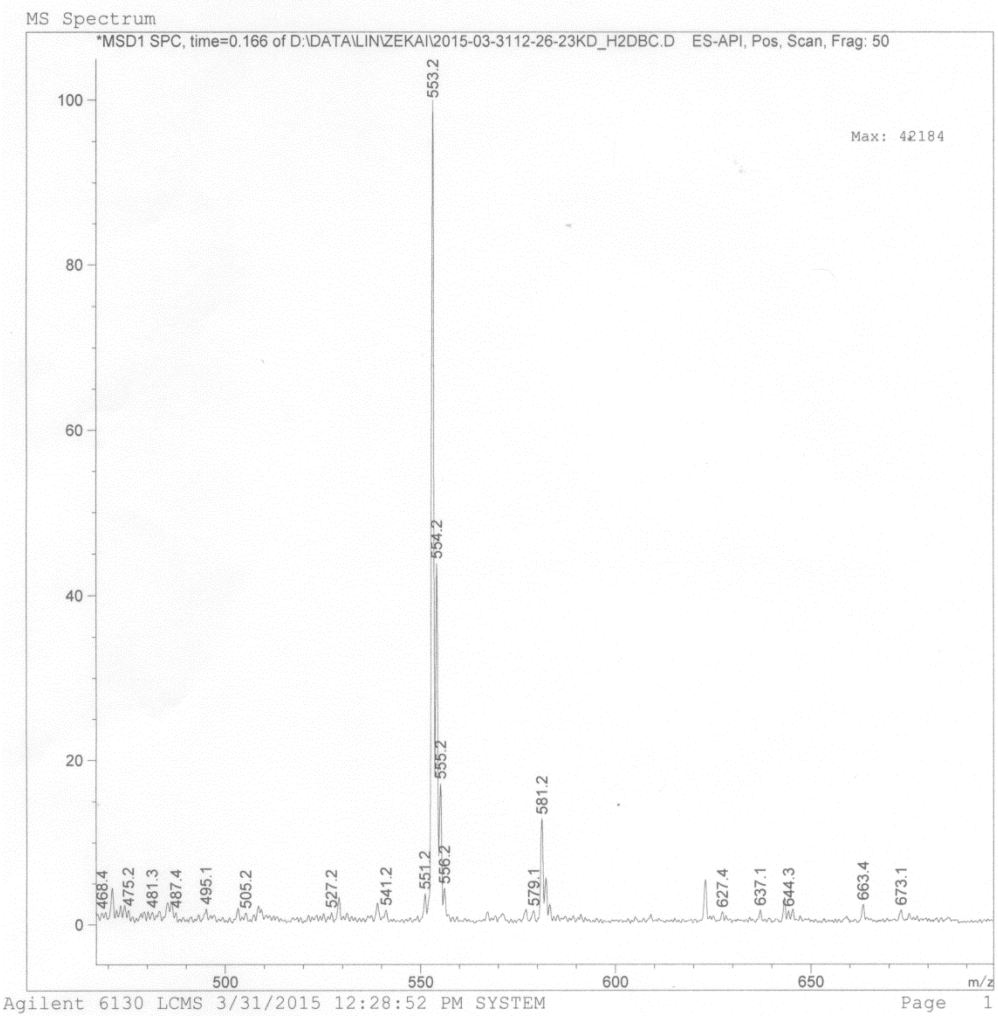

Figure S4 ESI-MS of 5, 15-di(p-benzoato)chlorin. The sample was prepared in DMSO as a 40 mg/L solution and was delivered by methanol.

3. Synthesis and characterization of the DBC-UiO NMOF

To a 20-mL glass vial was added 3 mL of $HfCl_4$ solution [2 mg/mL in N,N-dimethylformamide (DMF), 0.018 mmol], 3 mL of the H_2DBC solution (3.5 mg/mL in DMF, 0.018 mmol), and 0.36 mL of acetic acid (6.3 mmol). The reaction mixture was kept in an 80 °C oven for 3 days. The dark purple powder was collected by centrifugation and washed with DMF, triethylamine/ethanol (1:20 v/v), and ethanol.

The powder X-ray diffraction pattern of DBC-UiO matches that of DBP-UiO, despite that the DBC ligand has much lower symmetry than the DBP ligand. The DBC ligands are highly disordered (crystallographically) in the UiO framework. Based on ICP-MS and TGA results (below), DBP-UiO has a framework formula of $Hf_6(\mu_3\text{-}O)_4(\mu_3\text{-}OH)_4(DBP)_6$.

Thermogravimetric analysis on DBC-UiO NMOF was carried out on Shimadzu TGA-50 thermogravimetric analyzer. The sample was heated at 3 °C/min to 650 °C in air. The weight percentage was plotted against temperature (Figure S6). The weight loss in the 100 °C to 650 °C was 63.7 %, which is slightly lower than the calculated DBP ligand weight loss based

on the MOF formula (72 %). This discrepancy is presumably a result of the termination of $Hf_6(\mu_3\text{-}O)_4(\mu_3\text{-}OH)_4$ SBUs by acetate groups in the ultrathin DBC-UiO.

The Hf content in DBC-UiO was determined by inductively coupled plasma-mass spectrometry (ICP-MS, Agilent 7700x, USA). The NMOF sample was dried on vacuum overnight before being digested by concentrate nitric acid and hydrofluoric acid. The sample was diluted with 2% nitric acid to a total MOF concentration of 80 ppb. Hf concentration was determined to be 19.2 ppb thus Hf wt% in DBC-UiO was 24.0% (23.8% calculated). A plate-like morphology of DBC-UiO NMOF was confirmed by transmission electron microscopy (TEM, Tecnai F30 and Tecnai Spirit, FEI, USA). The particles display a plate-like morphology with thickness of 3-10 nm and plate diameter of 100~200 nm (Figure S7a). A tilt particle showing 4-fold symmetry diffraction pattern was also observed and the symmetry was confirmed by the FFT of a clip of the image (Figure S7b). Particle sizes of DBP-UiO NMOFs were determined to be 128.5 nm (PDI=0.17) by dynamic light scattering (DLS, Nano-ZS, Malvern, UK; Figure S8).

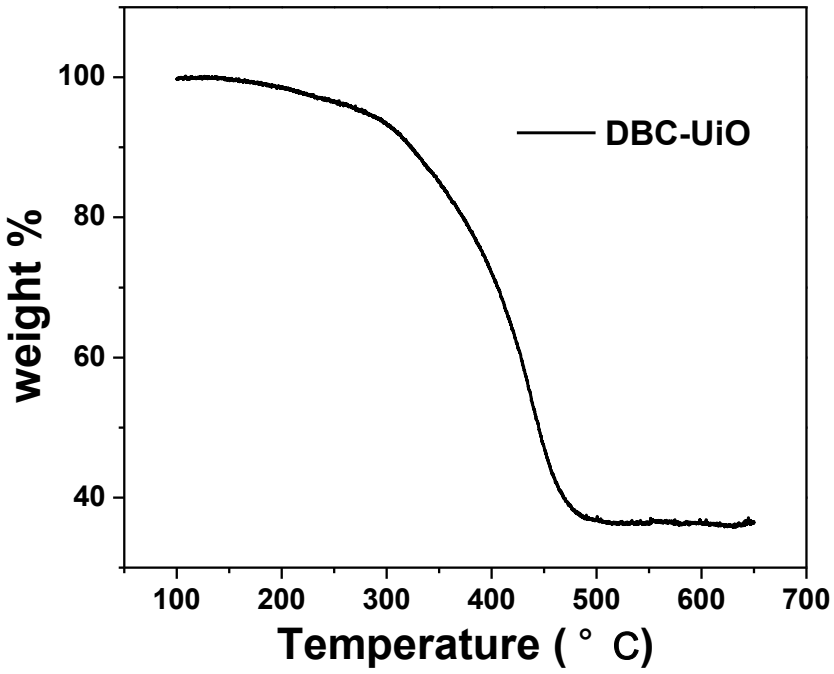

Figure S5 Thermogravimetric analysis of DBC-UiO.

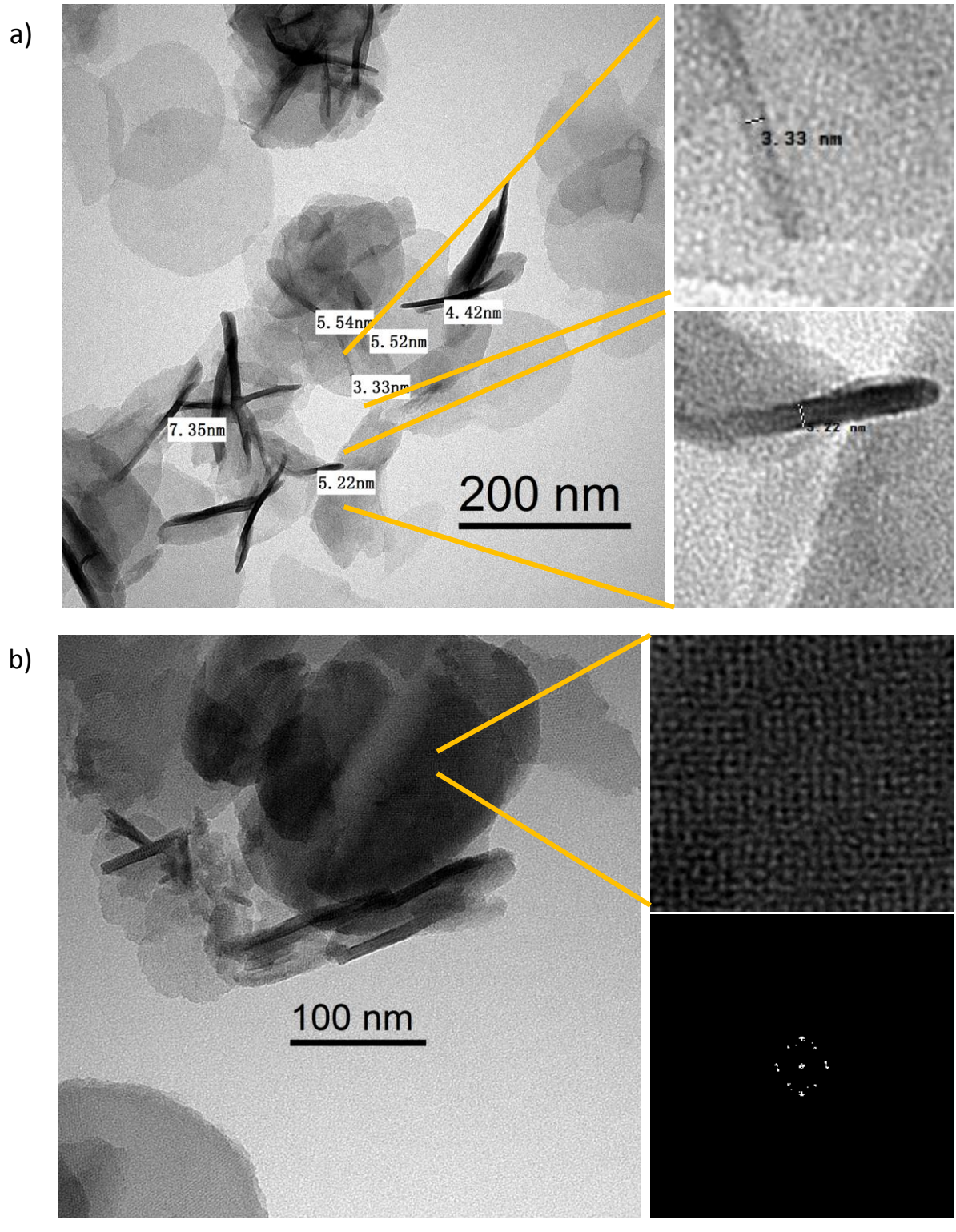

Figure S6 TEM images of DBC-UiO at different resolutions. (a) Left, a TEM image showing the thickness of the nanoplates lying perpendicular to the grid; right, zoomed-in view of two parts of the image showing the particles constructed from two (top) or three (bottom) packing layers. (b) TEM image showing a tilt particle (left) and the zoomed-in view of the NMOF (upper right) and its FFT showing 4-fold symmetry.

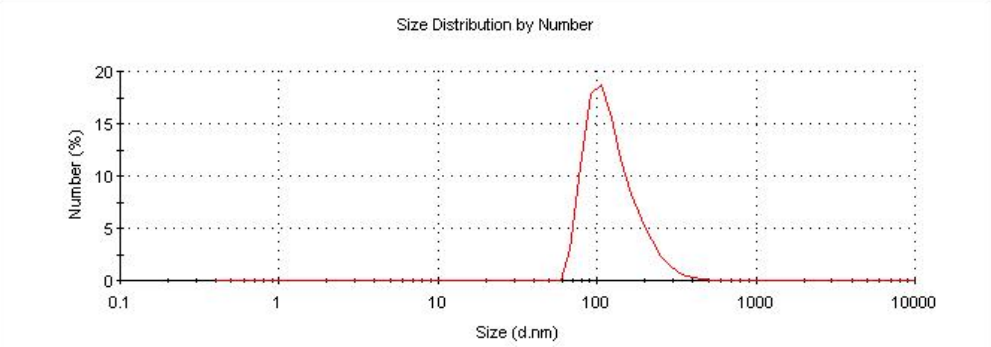

Figure S7 DLS plot showing the particle size of DBC-UiO.

4. Photochemical properties of H_2DBC and DBC-UiO

The UV-visible absorption spectra of H_2DBC and DBC-UiO were acquired with a UV-vis spectrophotometer (UV-2401PC, Shimadzu, Japan). H_2DBC and DBC-UiO NMOF were prepared as 4 μM (for PS concentration) solution/suspension in DMF or 0.67 mM phosphate buffer saline (PBS). The extinction coefficients of H_2DBC at 408 nm and 643 nm are 1.26×10^5 $M^{-1}cm^{-1}$ (Soret band) and 2.18×10^4 $M^{-1}cm^{-1}$(Q-band), respectively. The extinction coefficient of DBC-UiO at corresponding peaks are 1.09×10^5 $M^{-1}cm^{-1}$ (Soret band) and 2.46×10^4 $M^{-1}cm^{-1}$(Q-band), respectively. For DBC-UiO, the apparent extinction coefficient could be influenced by scattering and the broadening of Soret absorption.

The photostability of DBC-UiO and H_2DBC was monitored under LED irradiation (100 mW/cm2, 650 nm, Fig. S9). Solutions of 7.5 μM ligand or DBP-UiO (base on ligand concentration) were irradiated for 0, 0.5, 1, 2, 3, 5, 7 and 9 minutes and the concentrations were calculated from the characteristic absorption of chlorin species (Figure S10). DBC-UiO degraded much more slowly than the ligand and 87% of absorption was preserved after 9 min irradiation (54 J total light dose). In comparison, H_2DBC absorption preservation rate was only 76%.

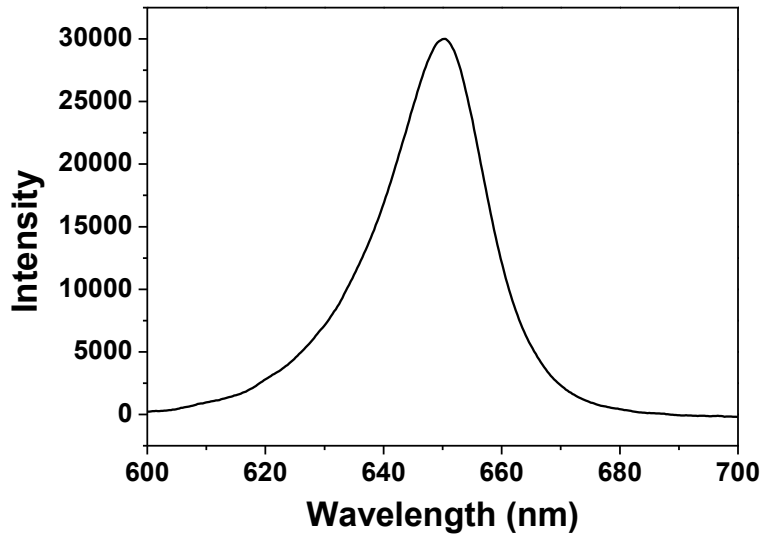

Figure S8 Emission spectrum of the 650 nm LED.

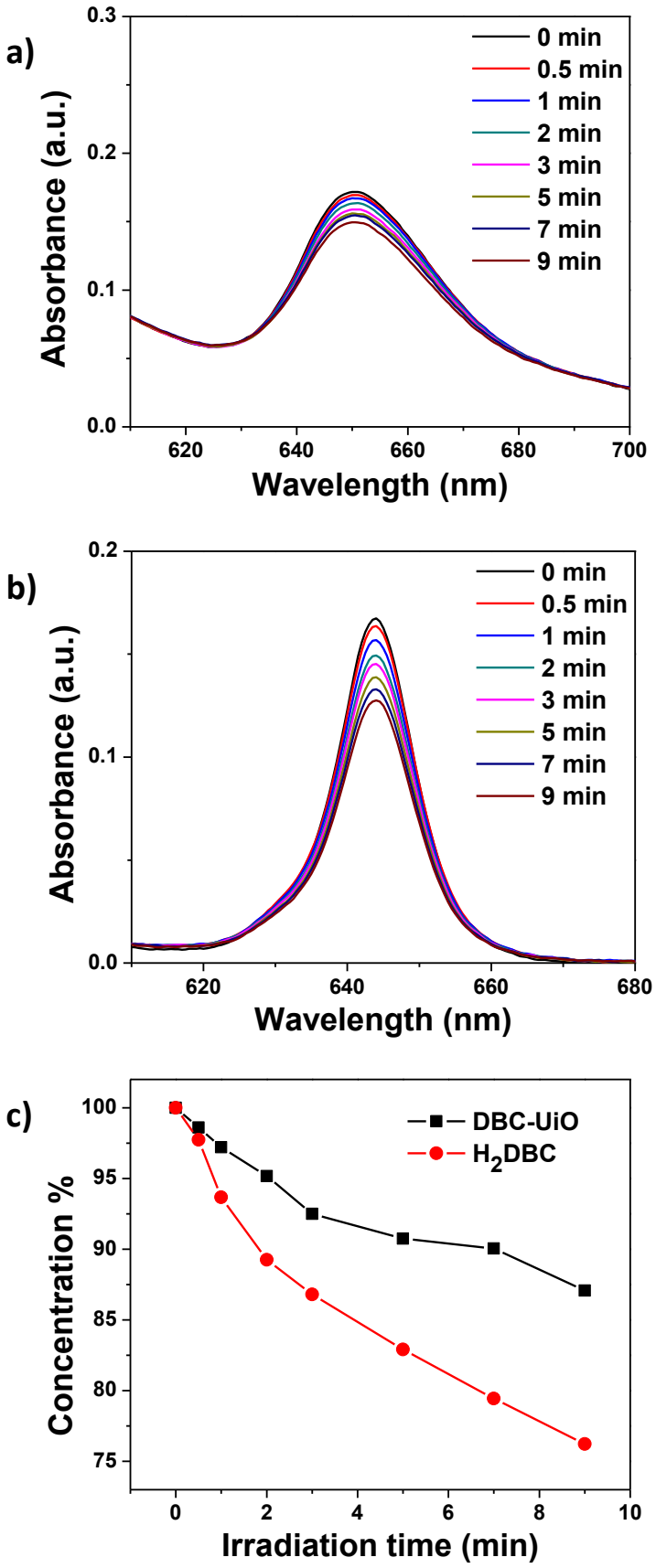

Figure S9 Photostability of DBC-UiO (a) and H_2DBC (b). (c) The dependence of the chlorin concentration of both DBC-UiO and H_2DBC on the irradiation time.

The fluorescence spectra of H_2DBC ligand and DBC-UiO NMOF were taken on a spectrofluorophotometer (Fluorolog-3, Horiba, Japan). H_2DBC was prepared into 1 μM solution in phosphate buffer saline and DBC-UiO was suspended in water to 1 μM (by ligand concentration). The ligand fluorescence peak appears at 641 nm with an intensity of $1.38*10^5$ (counts) while DBC-UiO fluorescence intensity was only 600~700 (counts) after correcting the background.

Time-domain lifetimes were measured on a ChronosBH lifetime fluorometer (ISS, Inc.) using Time-Correlated Single Photon Counting (TCSPC) methods. The fluorometer contained Becker-Hickl SPC-130 detection electronics and an HPM-100-40 Hybrid PMT detector. Excitation was provided by a 403nm picosecond pulsed laser source (Hamamatsu PLP-10). Emission wavelengths were selected with interference filters (Semrock). The Instrument Response Function (IRF) was measured to be approximately 0.009 ns FWHM in a 1% scattering solution of Ludox LS colloidal silica. Multi-component exponential decay lifetimes were fit via a forward convolution method in the Vinci control and analysis software. DBC-UiO, H_2DBC and a control mixture of Hf^{4+} and H_2DBC were prepared into solution/suspensions in HBSS or DMF (Figure S11). The fitted lifetimes are listed in Table S1.

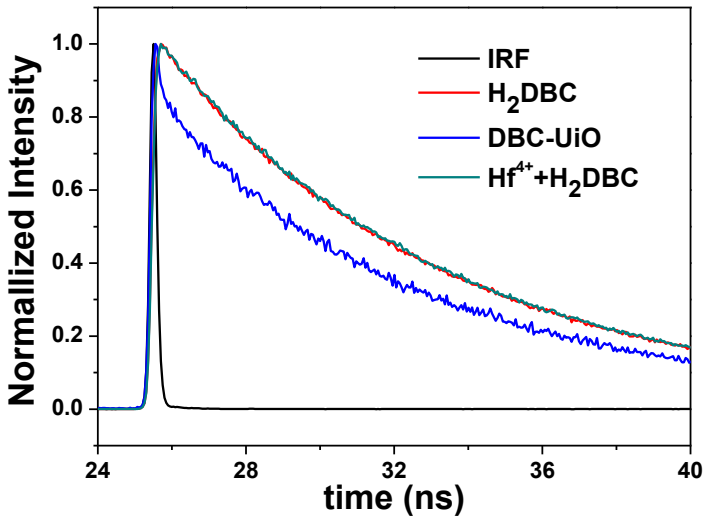

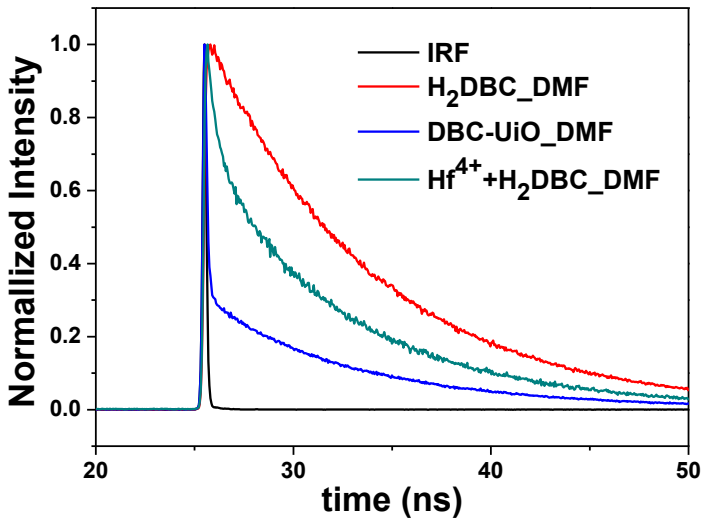

Figure S10 Time-resolved fluorescence decay traces of H_2DBC, DBC-UiO and a mixture solution of $HfCl_4$ and H_2DBC as a control in HBSS (top) and DMF (bottom), together with instrument response function (excitation/emission 408/640 nm).

Table S1 Lifetimes of H_2DBC, DBC-UiO and $HfCl_4$+DBC control fluorescence in different medium, fitted by software.

sample	τ_1 (ns)	τ_2 (ns)	τ_3 (ns)	$\bar{\tau}$ (ns)
IRF	0.0086	N/A	N/A	N/A
H_2DBC_HBSS	5.80	8.77	N/A	8.15
DBC-UiO_HBSS	3.27	8.26	0.14	7.88*
$HfCl_4$+DBC_HBSS	6.12	8.78	N/A	8.13
H_2DBC_DMF	8.27	N/A	N/A	N/A
DBC-UiO_DMF	3.24	8.54	0.19	8.16*
$HfCl_4$+DBC_DMF	2.41	7.97	0.38	7.32

* These average lifetimes are fitted with only τ_1 and τ_2, the τ_3 of these sets are known to be from scattering.

5. DBC-UiO stability in cell culture medium

The stability of DBC-UiO was tested by incubation of 0.5 mg DBC-UiO NMOF in RPMI 1640 medium for 12 hours. The NMOF was then collected by centrifugation and was washed with water. High-resolution TEM images and their fast Fourier transform patterns proved the crystallinity of DBC-UiO remained after incubation (Figure S12).

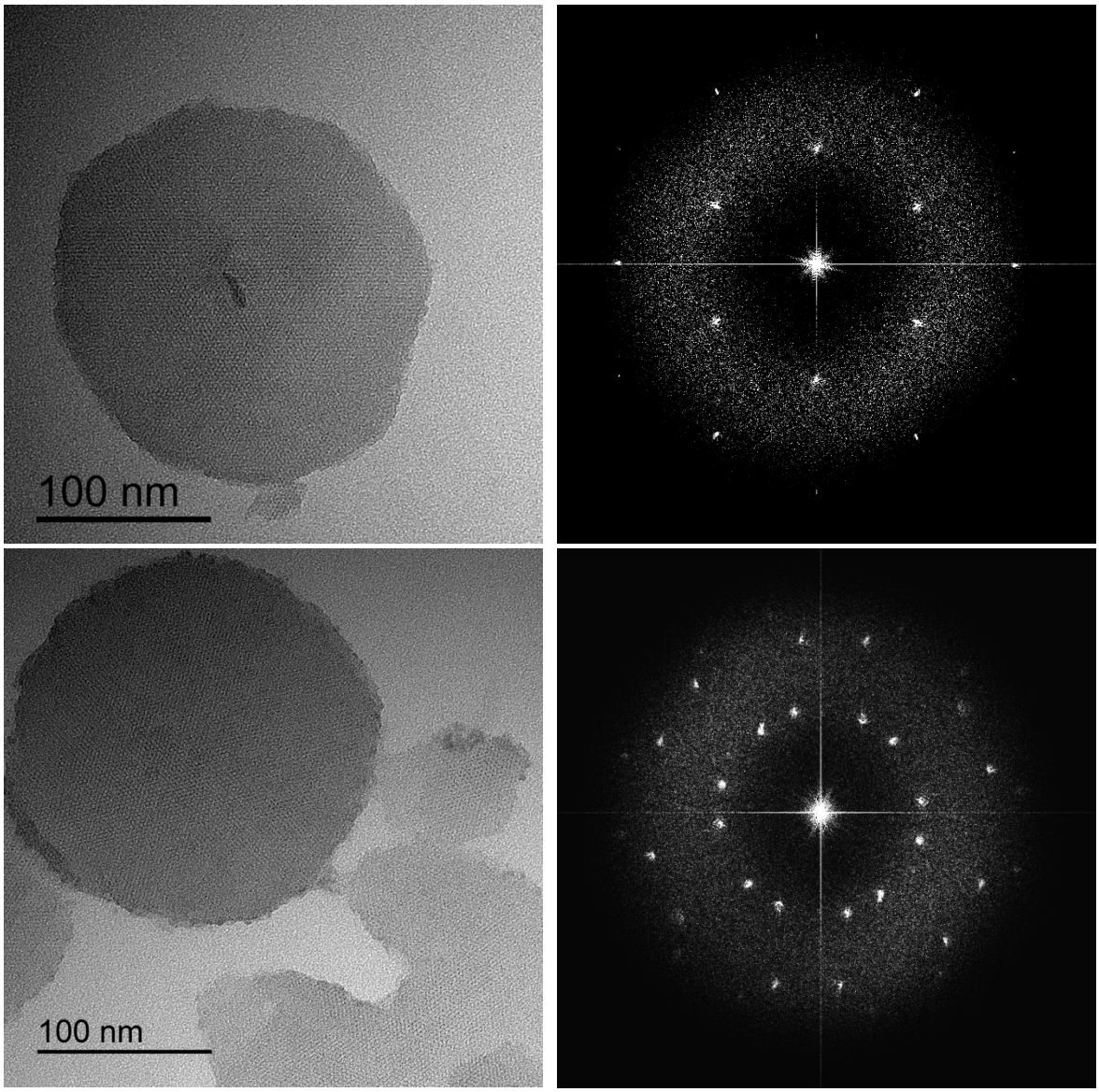

Figure S11 TEM image of DBC-UiO before (top left) and after (bottom left) cell culture medium cultivation and their FFT (right).

6. Singlet oxygen generation of H_2DBC and DBC-UiO

A light-emitting diode (LED) array with peak emission at 650 nm (Figure S14) was used as the light source of singlet oxygen generation test for H_2DBC and DBC-UiO while a 640 nm LED was used on H_2DBP, DBP-UiO and PpIX samples. The irradiance of LEDs are 100 mW/cm^2. Singlet oxygen sensor green (SOSG) reagent (Life Technologies) was employed for the detection of singlet oxygen. H_2DBC, DBC-UiO, H_2DBP, DBP-UiO and protoporphyrin IX (PpIX) samples were prepared in 1 μM solutions/suspensions in diluted HBSS buffer (for DBC-UiO and DBP-UiO, the concentration was calculated as ligand equivalents). To 2 mL each of these solutions/suspensions, SOSG stock solution (5 μL at 5 mM) was added (final concentration=12.5 μM) before fluorescence measurement.

For a typical measurement, fluorescence intensity was acquired on a spectrofluorophotometer (RF-5301PC, Shimadzu, Japan) with excitation at 504 nm and

emission at 525 nm (slit width 1.5 nm/3 nm for ex/em). Fluorescence was measured after irradiation by LED for 0 (as background), 15 s, 30 s, 45 s, 1 min, 1.5 min, 2 min, 3 min, 4 min, 5 min and 7 min.

7. Cellular uptake

DBP-UiO or DBC-UiO was incubated with CT26 cells at a Hf concentration of 50 μM for 4 h. The cells were collected, counted with a hemocytomter, and digested by concentrated nitric acid. The cellular uptake amounts of Hf were determined by ICP-MS and normalized with cell numbers.

H_2DBC or DBC-UiO was incubated with CT26 cells or HT29 cells at a ligand concentration of 5 μM for 4 h. The cells were collected, counted with a hemocytomter, redispersed in saturated K_3PO_4, and homogenized with an ultrasound probe. The ligand was further extracted by DMSO followed by centrifugation. The supernatant was subjected to UV-vis to determine the ligand concentration in the cells.

The cellular uptake amounts of DBC-UiO and H_2DBC in terms of ligand concentrations were (13.7±0.8) and (20.2±1.7) nmol/10^6 cells in HT29 cells (Figure S12) and (4.9±0.4) and (0.6±0.1) nmol/10^6 cells in CT26 cells (Figure S13). Although H_2DBC exhibited higher in vitro cellular uptake, its more profound photobleaching compared to DBC-UiO led to the less efficient cancer cell killing in HT29 cells. In CT26 cells, DBC-UiO showed significant higher cellular uptake than H_2DBC, which contributed to its more efficient cytotoxicity.

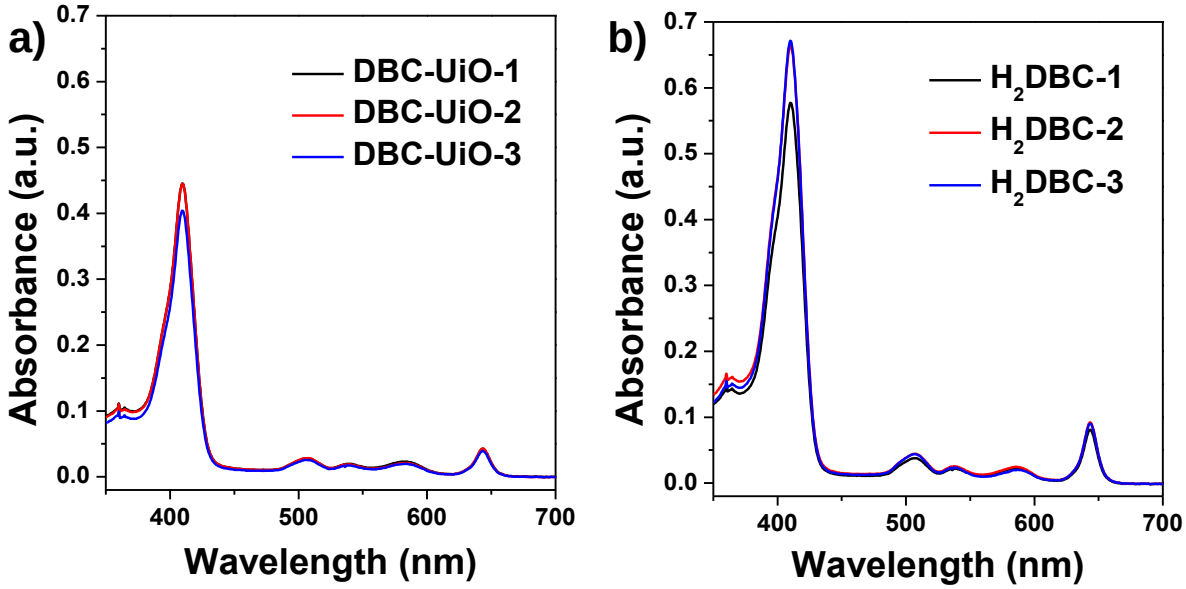

Figure S12 Cellular uptake of DBC-UiO (a) and H_2DBC (b) in terms of ligand concentrations in HT29 cells by UV-vis. Cells were incubated with DBC-UiO or H_2DBC at a ligand concentration of 5 μM for 4 h, homogenized by ultrasound probe, and subjected to UV-vis analysis after extracting the ligand by saturated K_3PO_4 and DMSO.

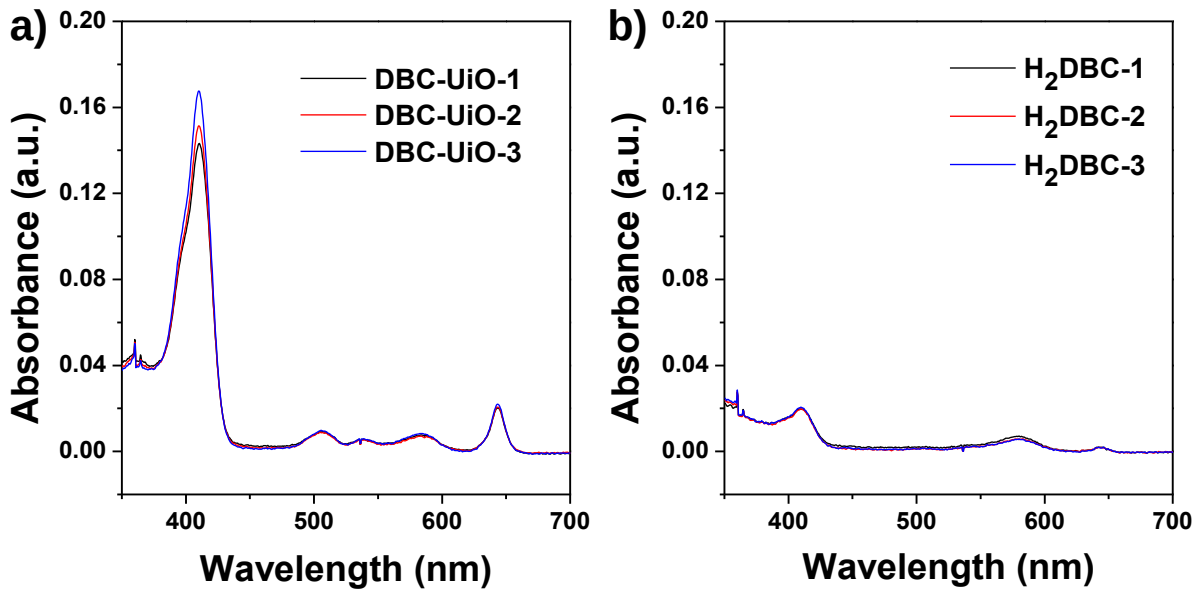

Figure S13 Cellular uptake of DBC-UiO (a) and H_2DBC (b) in terms of ligand concentrations in CT26 cells by UV-vis. Cells were incubated with DBC-UiO or H_2DBC at a ligand concentration of 5 μM for 4 h, homogenized by ultrasound probe, and subjected to UV-vis analysis after extracting the ligand by saturated K_3PO_4 and DMSO.

8. Cytotoxicity

The cytotoxicity of DBC-UiO, H_2DBC, DBP-UiO, and H_2DBP was evaluated in murine colorectal cancer cell CT26 and human colorectal cancer cell HT29 cells, respectively. CT26 cells and HT29 cells were seeded on 96-well plates at 1000 cells/well and 2500 cells/well, respectively. The cells were treated with DBC-UiO, H_2DBC, DBP-UiO, and H_2DBP at various ligand concentrations (2, 5, 10, and 20 μM base on ligand concentrations). A further incubation of 4 h was allowed followed by replacing the culture medium with 100 μL of fresh RPMI 1640 medium. The cells were irradiated with LED light (640 nm for DBC-UiO and H_2DBC; 630 nm for DBP-UiO and H_2DBP) at 100 mW/cm^2 for 15 min (total light dose 90 J/cm^2) or kept in dark, respectively. The cells were further incubated to achieve a total incubation time of 72 h. The cell viability was detected by (3-(4,5-dimethylthiazol-2-yl)-5-(3-carboxymethoxyphenyl)-2- (4-sulfophenyl)-2H-tetrazolium) (MTS) assay (Promega, USA).

In vitro cytotoxicity was also carried out in a murine macrophage Raw 264.7 cell line. Raw 264.7 cells were seeded on 96-well plates at 1000 cells/well. The cells were treated with DBC-UiO and H_2DBC at various ligand concentrations (2, 5, 10, 20, and 50 μM base on ligand concentrations). A further incubation of 4 h was allowed, followed by replacing the culture medium with 100 μL of fresh RPMI 1640 medium. The cells were irradiated with LED light (650 nm) at 100 mW/cm^2 for 15 min (total light dose 90 J/cm^2) or kept in dark, respectively. The cells were further incubated to achieve a total incubation time of 72 h. The cell viability was detected by MTS assay.

In Raw 264.7 cells, DBC-UiO significantly outperformed H_2DBC in cell killing as shown

in Figure S14. Higher concentrations of DBC-UiO and H_2DBC are required to achieve efficient macrophage killing compared to colorectal cancer cells including CT26 and HT29.

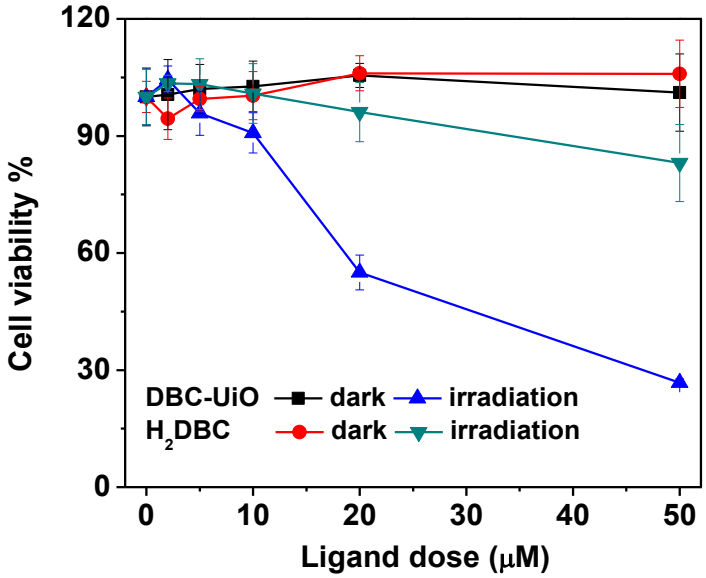

Figure S14 In vitro PDT cytotoxicity of DBC-UiO and H2DBC at different PS concentrations in murine macrophage Raw 264.7 cells.

9. Mechanisms of cytotoxicity

9.1. Apoptosis and necrosis

The apoptosis and necrosis induced by PDT of DBC-UiO and H_2DBC were evaluated by flow cytometry. CT26 cells were seeded at 1×10^6 cells per well in 6-well plates and further cultured for 24 h. The culture media were replaced by 2 mL of fresh culture media containing 10% FBS. DBC-UiO and H_2DBC were added to the cells, respectively, at an equivalent ligand concentration of 5 μM. Cells incubated with PBS served as control. After 24-h incubation, the cells were irradiated with LED light (650 nm) at 100 mW/cm^2 for 15 min (equals to 90 J/cm^2). Following further incubation of 24 h, the floating and adherent cells were collected and stained with Alexa Fluor 488 Annexin V/dead cell apoptosis kit (Invitrogen, USA) according to manufacturer's instructions. The apoptosis and necrosis was examined on a flow cytometer (LSRII Orange, BD, USA).

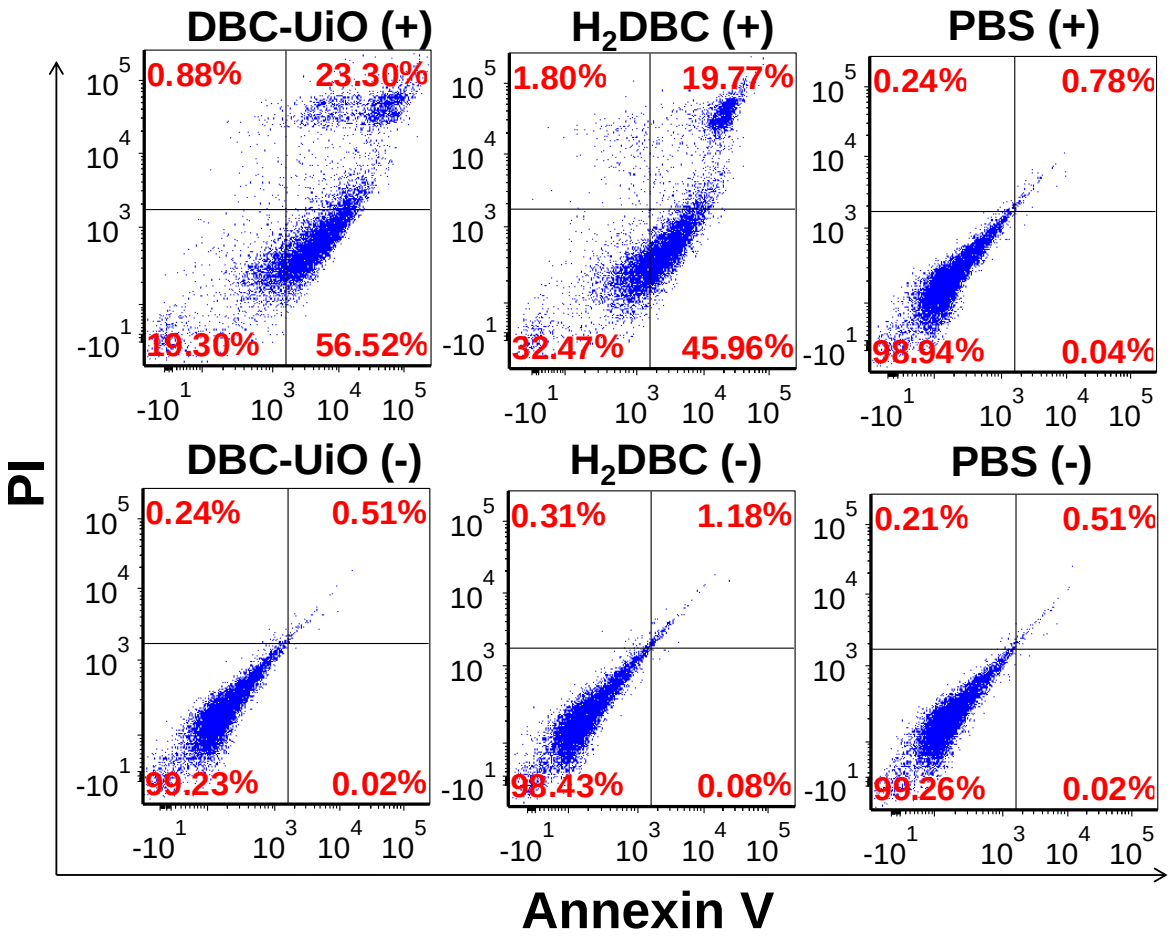

Figure S15 Annexin V/PI analysis of CT26 cells incubated with DBC-UiO, H_2DBC, or PBS with or without irradiation (90 J/cm^2). The quadrants from lower left to upper left (counter clockwise) represent healthy, early apoptotic, late apoptotic, and necrotic cells, respectively. The percentage of cells in each quadrant was shown on the graphs. (+) and (-) refer to with and without irradiation, respectively.

9.2. Immunogenic cell death

The immunogenic cell death by PDT of DBC-UiO and H_2DBC were evaluated by immunofluorescence and flow cytometry. For immunofluorescence analysis, CT26 cells were seeded at 5×10^5 cells per well in 6-well plates and further cultured for 24 h. The culture media were replaced by 2 mL of fresh culture media containing 10% FBS. DBC-UiO and H_2DBC were added to the cells, respectively, at an equivalent ligand concentration of 5 μM. Cells incubated with PBS served as control. After 24-h incubation, the cells were irradiated with LED light (650 nm) at 100 mW/cm^2 for 15 min (equals to 90 J/cm^2). Following further incubation of 4 h, the cells were washed with PBS three times, fixed with 4% paraformaldehyde, incubated with AlexaFluor 488-calreticulin (CRT) antibody for 2 h, stained with DAPI, and observed under CLSM using 405 nm and 488 nm lasers for visualizing nuclei and CRT expression on the cell membrane, respectively.

For flow cytometry analysis, CT26 cells were seeded at 1×10^6 cells per well in 6-well plates and further cultured for 24 h. The culture media were replaced by 2 mL of fresh culture media containing 10% FBS. DBC-UiO and H_2DBC were added to the cells, respectively, at

an equivalent ligand concentration of 5 μM. Cells incubated with PBS served as control. After 24-h incubation, the cells were irradiated with LED light (650 nm) at 100 mW/cm^2 for 15 min (equals to 90 J/cm^2). Following further incubation of 4 h, the cells were collected, incubated with AlexaFluor 488-CRT antibody for 2 h, and stained with propidium iodide (PI). The samples were analyzed by flow cytometer (LSRII Orange, BD, USA) to identify cell surface CRT. The fluorescence intensity of stained cells was gated on PI-negative cells.

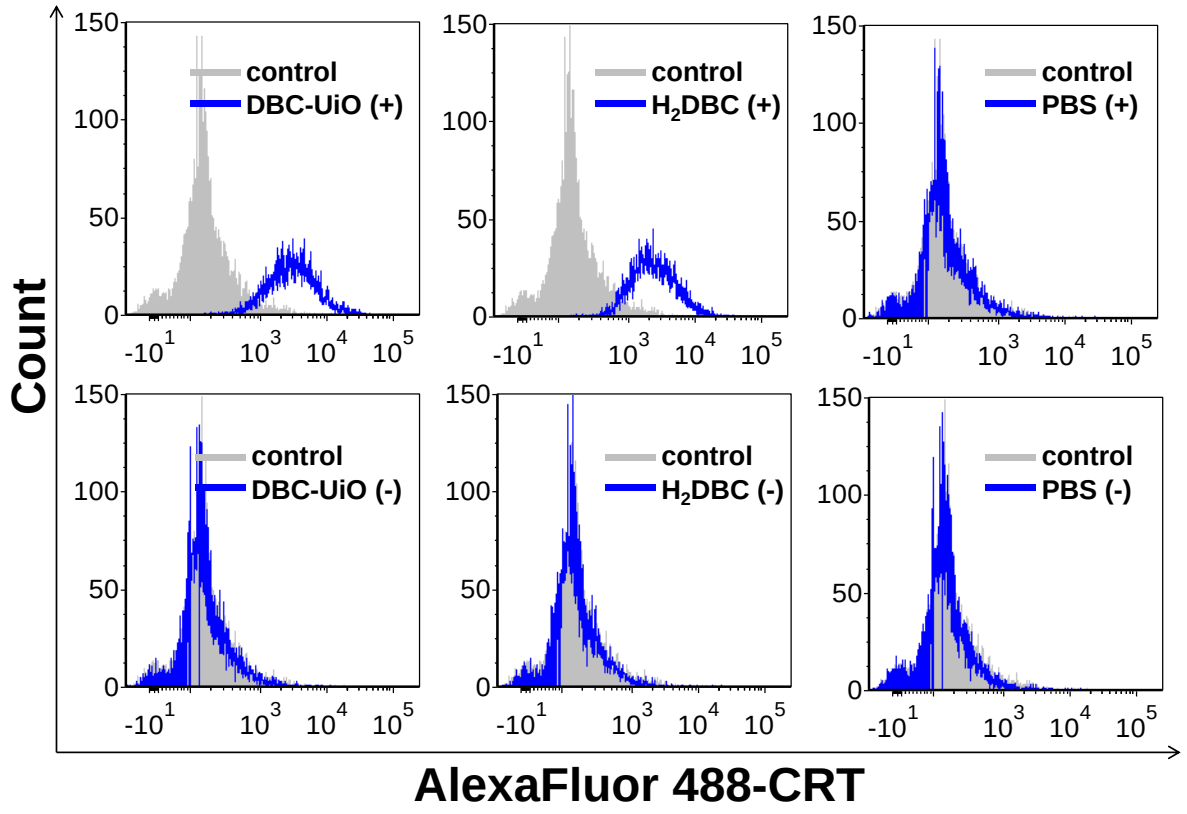

Figure S16 CRT exposure determines the immunogenicity of PDT induced cell death. CRT exposure on the cell surface of CT26 cells was assessed after incubation with DBC-UiO, H_2DBC, or PBS with or without light irradiation (90 J/cm^2) by immunofluorescence staining followed by flow cytometry analysis. The fluorescence intensity was gated on PI-negative cells.

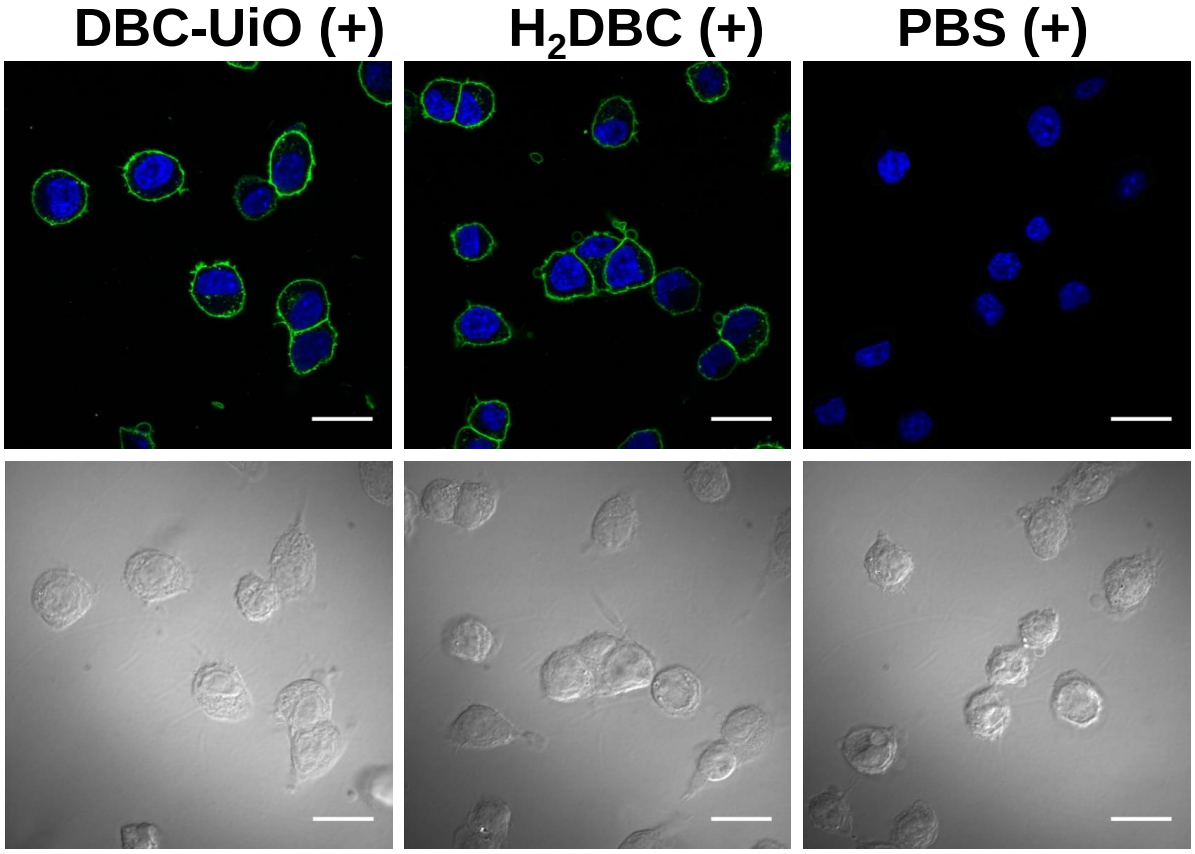

Figure S17 Immunofluorescence microscopy of CRT expression on the cell surface of CT26 cells treated with DBC-UiO and PBS upon irradiation (90 J/cm^2). Blue: DAPI stained nuclei; Green: Alexa Fluor 488-CRT antibody. Bar=20 μm.

10. In vivo anticancer efficacy

The PDT efficacy of DBC-UiO was investigated using a flank CT26 mouse tumor model and HT29 subcutaneous xenograft mouse model. Tumor bearing mice were established by subcutaneous inoculation of HT29 cell suspension (2×10^6 cells per mouse) or CT26 cell suspension (1×10^6 cells per mouse) into the right flank region of 6-week athymic male nude mice or 6-week BALB/c male mice, respectively. Six groups were included for comparison: (1) PBS control, (2) DBC-UiO, (3) DBP-UiO, (4) H_2DBC, or (5) H_2DBP at a ligand dose of 1 mg/kg or (6) DBC-UiO at a ligand dose of 3.5 mg/kg. Twelve hours post injection, each mouse in group (1)- (5) was irradiated at the tumor site with light (0.1 W/cm^2) for 15 min (90 J/cm^2) and the mice in group (6) received light irradiation (0.1 W/cm^2) for 30 min (180 J/cm^2). For (1) to (5) groups on the CT26 model, mice are treated again 4 days after first treatment, while for (1) to (5) groups on HT29 model, mice are treated every 4 days for total 4 treatments. When tumors reached 100 mm^3, PBS, DBC-UiO, DBP-UiO, H_2DBC, or H_2DBP were intratumorally injected to animals. At 12 h post-injection, mice were anesthetized with 2% (v/v) isoflurane and tumors were irradiated with a 640 nm LED for DBP-UiO or a 650 nm LED for DBC-UiO. The light intensity was measured as 100 mW/cm^2.

To evaluate the therapeutic efficacy, tumor growth and body weight evolution were

monitored. The tumor size was measured with a digital caliper every day. Tumor volumes were calculated as follows: (width^2 × length)/2. Finally, all mice were sacrificed when the tumor size of control group exceeded 2 cm^3, and the excised tumors were photographed and weighed. The tumors were embedded in optimal cutting temperature (OCT) medium, sectioned at 5-μm thickness, and subjected to hematoxylin and eosin (H&E) stain for histopathological analysis.

The statistical analysis of tumor weights was run by two-way T-test. For CT26 model, the *P* values of DBC-UiO, DBC-UiO (higher dose), DBP-UiO, H_2DBC, and H_2DBP vs. PBS are 0.00001, 0.000004, 0.20656, 0.06635, and 0.43296, respectively. For HT29 model, the *P* values of DBC-UiO, DBC-UiO (higher dose), DBP-UiO, H_2DBC, and H_2DBP vs. PBS are 0.0000005, 0.000000008, 0.43374, 0.07042, and 0.15008, respectively. Significant difference of tumor weights was only observed between DBC-UiO and PBS control group. DBC-UiO with higher doses of NMOF and light irradiation led to successful tumor regression in both models.

Table S2 Statistical analysis of tumor weights by t-test shown with P values.

	CT26 tumor model	HT29 tumor model
DBC-UiO vs. PBS	0.00001	0.0000005
DBP-UiO vs. PBS	0.20656	0.43374
H2DBC vs. PBS	0.06635	0.07042
H2DBP vs. PBS	0.43296	0.15008
DBC-UiO (higher dose) vs. DBC-UiO	0.000004	0.000000008
DBC-UiO vs. DBC-UiO (higher dose)	0.000441	0.000000054

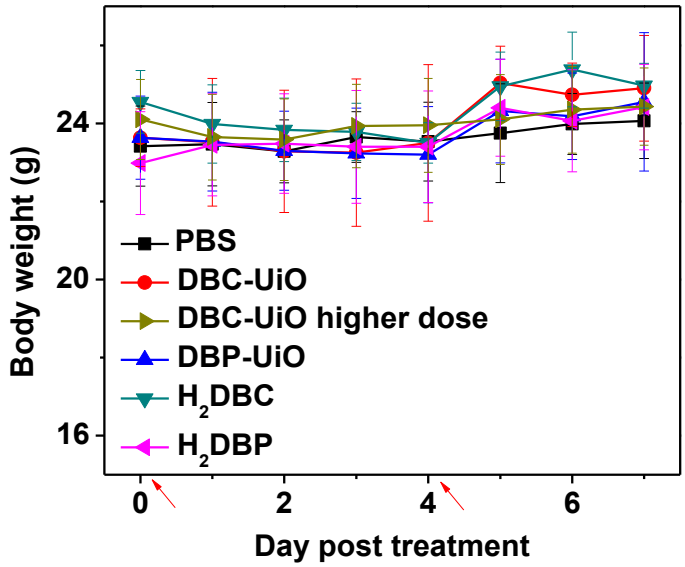

Figure S18 Body weight evolution of CT26 tumor bearing BALB/c mice treated with NMOF and PS ligands (n=6).

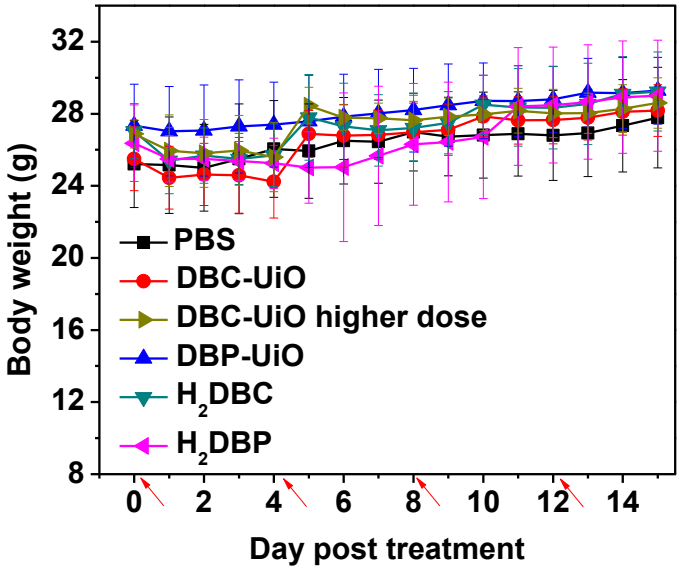

Figure S19 Body weight evolution of HT29 tumor bearing nude mice treated with NMOF and PS ligands (n=6).

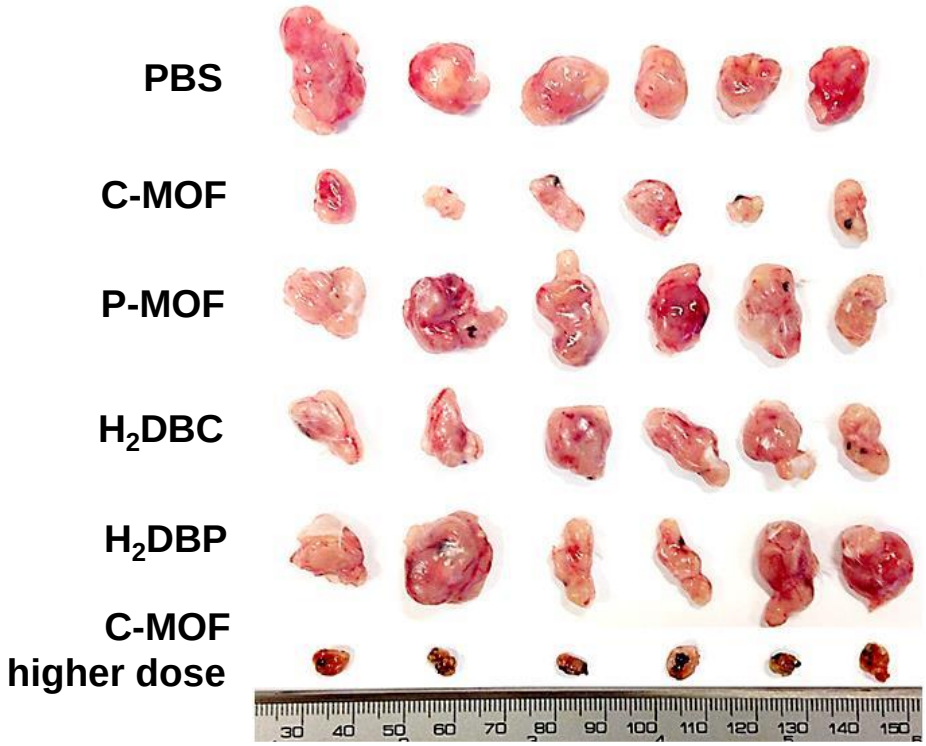

Figure S20 Photos of excised tumors of each group after PDT treatment in the CT26 model.

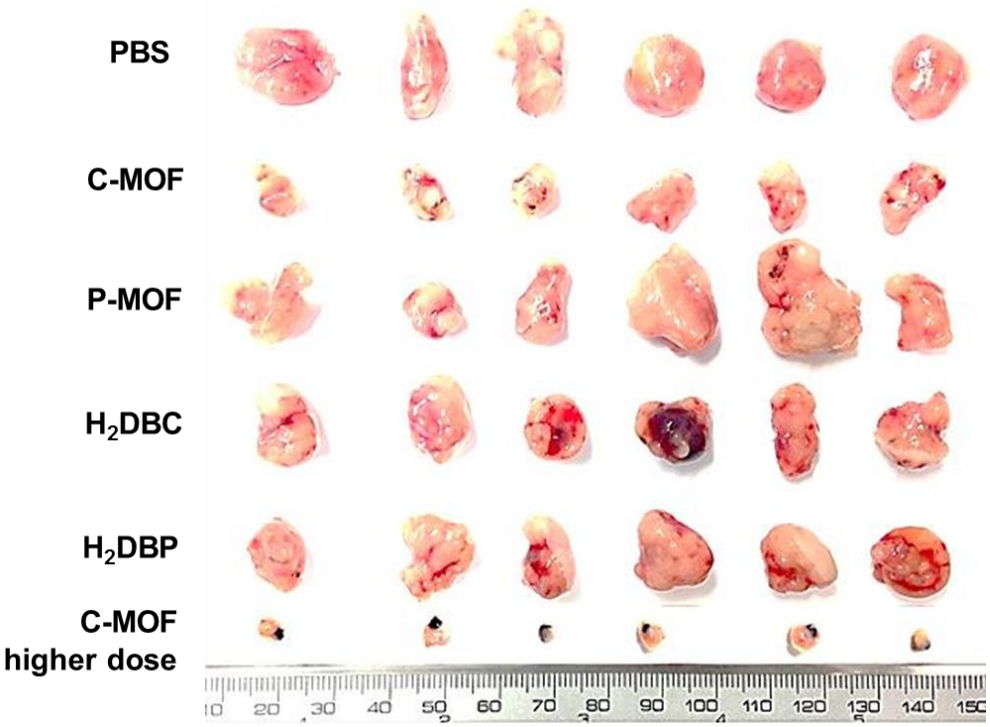

Figure S21 Photos of excised tumors of each group after PDT treatment in the HT29 model.

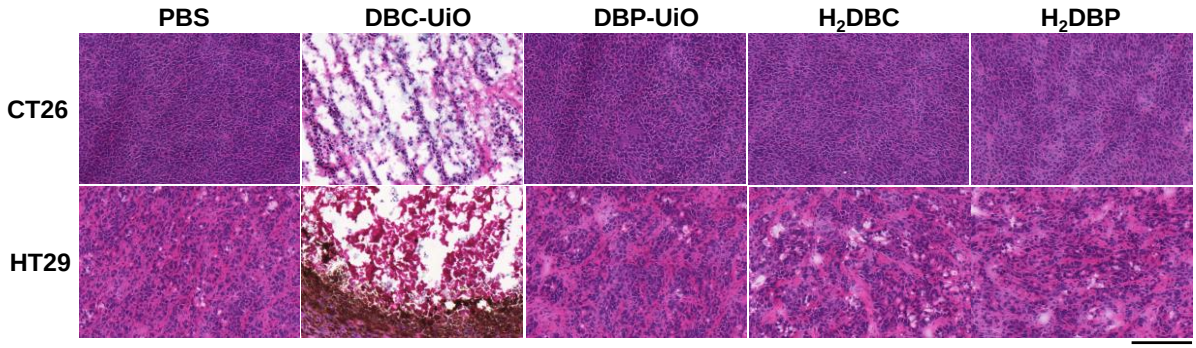

Figure S22 Histology of frozen tumor tissue slices after H-E staining. Bar=100 μm.

11. References

(1) Lu, K.; He, C.; Lin, W. *Journal of the American Chemical Society* **2014**, *136*, 16712.
(2) Wang, T. Y.; Chen, J. R.; Ma, J. S. *Dyes and pigments* **2002**, *52*, 199.